Cluster expansions in the (2+1)D Ising model

1984 J. Phys. A: Math. Gen. 17 1649

(http://iopscience.iop.org/0305-4470/17/8/021)

J. Phys. A: Math. Gen. **17** (1984) 1649–1664. Printed in Great Britain

Cluster expansions in the (2+1)D Ising model

C J Hamer and A C Irving†

Department of Theoretical Physics, Research School of Physical Sciences, The Australian National University, Canberra, ACT 2601, Australia

Received 18 October 1983, in final form 16 December 1983

Abstract. The cluster expansion methods of Nickel are applied to calculate high-temperature series for the vacuum energy and specific heat, the susceptibility, and the mass gap in the (2+1)D Ising model. Critical points and critical exponents are estimated for the square and triangular lattices. The results demonstrate universality with the 3D Ising model, within errors. Exact linked cluster expansions are formulated for the quantities above, and their convergence and scaling properties are investigated.

1. Introduction

Linked cluster expansions are the most efficient method presently known for generating perturbation series in Hamiltonian field theory. This method was originally proposed by Nickel (1980a), and applied to the ground-state properties of the (2+1)D Ising model in the low-temperature regime by Marland (1981). In a pair of recent papers, we have derived a connected diagram expansion (Hamer and Irving 1984) which is essentially equivalent to Nickel's expansion; and applied the linked cluster method to Z_2 and U(1) gauge theories in (2+1)D, extending the approach to calculate the axial string tension as well as the ground-state energy (Irving and Hamer 1983a, hereafter referred to as I).

In the present work, the approach is applied to the (2+1)D Ising model in the high-temperature regime. High-temperature series are calculated for the ground-state properties (specific heat and susceptibility) on square and triangular lattices. Another algorithm due to Nickel (1980a), this time involving both linked and unlinked clusters, is used to generate series for the mass gap. Using Padé approximant methods, the critical point parameters are estimated as $x_c = 0.20976 \pm 0.00015$, $\gamma = 1.247 \pm 0.005$ and $\nu = 0.64 \pm 0.02$ for the triangular lattice, and $x_c = 0.3290 \pm 0.001$, $\gamma = 1.257 \pm 0.01$ and $\nu = 0.66 \pm 0.02$ for the square lattice. These results are in good agreement with previous estimates (Marland 1981, Elliott *et al* 1970, Pfeuty and Elliott 1971, Yanase *et al* 1976, Jullien *et al* 1978, Penson *et al* 1979, Hamer 1983), and confirm universality of the indices γ and ν with the 3D Ising model, within errors.

An *exact* linked cluster expansion (ELCE), which was proposed in I, is also applied to the model. In this approach, the contribution of each cluster is evaluated exactly, rather than being expanded as a power series. The method is extended to the case of the mass gap, and the convergence and scaling properties of the ELCE approximants are investigated. It is shown that quite good estimates of the critical parameters can

† Permanent address: DAMTP, University of Liverpool, Liverpool L69 3BX, UK.

0305-4470/84/081649+16$02.25

be extracted from the scaling behaviour of the ELCE approximants near the critical point, but that the method will usually be inferior to series (Gaunt and Guttmann 1974) and finite-lattice methods (Hamer 1983, Hamer and Barber 1981b) in this respect. The method should prove useful, nevertheless, for confining gauge theories in the weak-coupling regime (Irving and Hamer 1983a, b), where finite-lattice calculations are hardly feasible, and series approximants break down.

2. The vacuum energy and its derivatives

The Hamiltonian of the (2+1)D Ising model may be written in the 'high-temperature' representation as (Fradkin and Susskind 1978):

$$H = \sum_m (1 - \sigma_3(m)) - x \sum_{m,\hat{\mu}_i} \sigma_1(m)\sigma_1(m+\hat{\mu}_i) - h \sum_m \sigma_1(m). \tag{2.1}$$

Here the index m labels sites on a two-dimensional spatial lattice, and $\{\hat{\mu}_i\}$ are its two unit base vectors, while the time variable is continuous. The σ_i are Pauli matrices acting on a two-state spin variable at each site, x is the coupling (analogous to the inverse temperature β in the Euclidean formulation), and h is a magnetic field variable. We are interested in calculating the lowest two eigenvalues ω_0 and ω_1 of the Hamiltonian (2.1). Quantities derived therefrom are the ground-state energy per site, ω_0/N, where N is the number of sites of the lattice; the mass gap

$$F(x) = \omega_1(x) - \omega_0(x); \tag{2.2}$$

the 'specific heat' (Hamer and Barber 1981a)

$$\tilde{C}(x) = -(x^2/N)(\partial^2\omega_0/\partial x^2); \tag{2.3}$$

and the magnetic susceptibility

$$\chi(x) = -(1/N)(\partial^2\omega_0/\partial h^2). \tag{2.4}$$

2.1. Linked cluster method

In I we have discussed a linked cluster expansion, originally proposed by Nickel (1980a) and implemented by Marland (1981), which is applicable to the ground-state energy. The vacuum energy per site for an infinite lattice may be expressed in the form

$$\lim_{N\to\infty}\left\{\frac{\omega_0}{N}\right\} = \sum_{(m,\alpha_m)} l_{m,\alpha_m}\varepsilon_{m,\alpha_m}, \tag{2.5}$$

where the sum runs over all topologically distinct linked clusters (m, α_m) consisting of m points arranged in configuration α_m, $m = 1, 2, \ldots, \infty$. The number l_{m,α_m} is an integer lattice constant (Domb 1960, 1974), namely the number of ways in which the cluster (m,α_m) can be embedded on the lattice, divided by the number of sites N. The quantity ε_{m,α_m} is the contribution made by a cluster (m,α_m) to the vacuum energy, and is equivalent in perturbation theory (Hamer and Irving 1984) to the sum of all connected diagrams which span the cluster.

The most convenient way to calculate the quantities ε_{m,α_m} is by an iterative method, starting from the smallest clusters and working upwards. The ground-state energy for any given cluster (i, α_i) with free boundaries can be expressed, like that of the infinite

lattice, as a sum of contributions from each embedded sub-cluster, thus:

$$\omega_0^{i,\alpha_i} = \sum_{(j,\alpha_j)} C_{j,\alpha_j}^{i,\alpha_i} \varepsilon_{j,\alpha_j} \tag{2.6}$$

where $C_{j,\alpha_j}^{i,\alpha_i}$ is the embedding constant (Domb 1960, 1974), or number of ways in which the sub-cluster (j, α_j) can be embedded in (i, α_i). Efficient techniques have been developed previously (Hamer and Barber 1981a, Roomany and Wyld 1980, Hamer 1983) for calculating the energies ω_0^{i,α_i}; and then it is a simple matter to invert the relations (2.6) and calculate the ε_{j,α_j} for progressively larger clusters.

In I the calculation of the vacuum energy for the Z_2 gauge model in (2+1)D was discussed, where the linked clusters consist of adjoining 'plaquettes', and the lattice constants required are low-temperature or 'strong' embedding constants (Domb 1960, 1974)—that is, lattice embeddings in which two plaquettes are adjacent to each other are not allowed unless the two plaquettes are also adjacent in the original topology (j, α_j). In the present case, the relevant topologies consist of clusters of sites joined by links (on which the spin-flip operators $\sigma_1(m)\sigma_1(m+\hat{\mu}_i)$ may act), and the lattice constants required are the high-temperature or 'weak' embedding constants. The calculation of these constants is discussed in appendix 1.

2.2. *Series results and analysis*

Our first use of the linked cluster method is to calculate series expansions for the vacuum energy in powers of x and h. Then the quantities ω_0^{i,α_i} and ε_{j,α_j} are themselves expressed as series in x and h; and to calculate the susceptibility to order x^M, say, it is sufficient to consider clusters of m sites with $m \leq M+1$, because a connected diagram of order M cannot span any larger cluster.

Table 1. High-temperature series in x for the vacuum energy per site, ω_0/N, the susceptibility χ and the mass gap F of the (2+1)D Ising model. Coefficients at order M are listed for the square and triangular lattices.

M	ω_0/N	χ	F
Square lattice			
0	0	1	2
1	0	4	−4
2	−0.5	13.5	−2
3	0	45	−3
4	−0.468 75	144.843 75	−4.5
5	0	464.444 444 444	−11
6	−1.148 437 5	1469.358 506 94	−20.507 8125
7	0	4639.482 349 54	
Triangular lattice			
0	0.	1	2
1	0.	6	−6
2	−0.75	32.25	−6
3	−0.75	166.5	−10.5
4	−1.359 375	843.046 875	−31.5
5	−3.093 75	4 218.416 666 67	−98.531 25
6	−8.355 468 75	20 941.023 003 5	−346.710 9375

Expansions have been derived for the vacuum energy and susceptibility as functions of x, up to sixth order for the triangular lattice and seventh order for the square lattice. The results are shown in table 1. The calculation for the triangular lattice took approximately 20 minutes on a VAX 11/780, and was increasing by a factor of three or so for each order in x: so one may contemplate extending these series by several more orders on a large mainframe computer. In fact, Yanase *et al* (1976) have previously calculated the susceptibility of the model (2.1) to seventh order, by a connected diagram method, but did not publish their series coefficients explicitly. For comparison, we may note that Nickel (1980b) has calculated the susceptibility for the 3D Euclidean Ising model to $O(\beta^{21})$. In diagrammatic terms (Hamer and Irving 1984), one order in x is equivalent to two in β, but still our results are only equivalent to $O(\beta^{12})$ or $O(\beta^{14})$.

These series have been analysed by the standard method of Padé approximants (Gaunt and Guttmann 1974). As is well known, the high-temperature susceptibility series is extremely smooth and well behaved, and one obtains accurate estimates of the critical parameters (table 2):

$$\left.\begin{aligned} x_c &= 0.20976 \pm 0.00015 \\ \gamma &= 1.247 \pm 0.005 \end{aligned}\right\} \tag{2.7}$$

for the triangular lattice, and

$$\left.\begin{aligned} x_c &= 0.3290 \pm 0.001 \\ \gamma &= 1.257 \pm 0.01 \end{aligned}\right\} \tag{2.8}$$

Table 2. Padé analysis of the series for $D \log \chi$ in the $(2+1)$D Ising model. Listed are the position and residue (in parentheses) of the leading pole on the real axis in the $[N/M]$ Padé approximant to this series. Our resulting estimates of the critical parameters are shown below.

Order of Padé N	$[N/N-1]$	$[N/N]$	$[N/N+1]$
Square lattice			
1		0.297 3 (0.972)	0.327 9 (1.245)
2	0.359 7 (1.721)	0.329 5 (1.264)	0.329 1 (1.258)
3	0.328 9 (1.255)		
	Estimate: $x_c = 0.329\,0 \pm 0.001$, $\gamma = 1.257 \pm 0.01$		
Triangular lattice			
1		0.211 1 (1.270)	0.210 69 (1.264)
2	0.209 61 (1.243)	0.209 75 (1.247)	0.209 76 (1.247)
3	0.209 76 (1.247)		
	Estimate: $x_c = 0.209\,76 \pm 0.000\,15$, $\gamma = 1.247 \pm 0.005$		

for the square lattice. These results for the critical couplings x_c are in close agreement with the ratio method estimates of Yanase *et al* (1976), namely 0.2098 and 0.3285 for triangular and square lattices, respectively. The series for the specific heat are shorter, and the Padé results less stable, giving critical parameter estimates of very little value: we shall not present them here.

2.3. Exact linked cluster expansion

This technique (ELCE) was introduced in I. One still makes use of the linked cluster expansions (2.5) and (2.6), but now the quantities ω_0^{i,α_i} and ε_{j,α_j} are calculated *exactly*, by matrix diagonalisation methods (Hamer and Barber 1981a, Roomany and Wyld 1980) such as the Lanczos algorithm, and then the sum (2.5) is evaluated, including all clusters up to some convenient maximum size $m = M$. For any given coupling x and magnetic field h, one thus obtains a sequence of approximations to the vacuum energy per site, which we expect to converge to the exact bulk value in the limit $M \to \infty$. One can easily deduce corresponding values for the specific heat and susceptibility.

Figures 1(a) and (b) display some results of this sort for the specific heat and susceptibility of the triangular lattice, as a function of cut-off L, where L is the number of links in the cluster. Also shown for comparison is a high-order Padé approximant derived from the series expansions in table 1. It can be seen that the sequence of

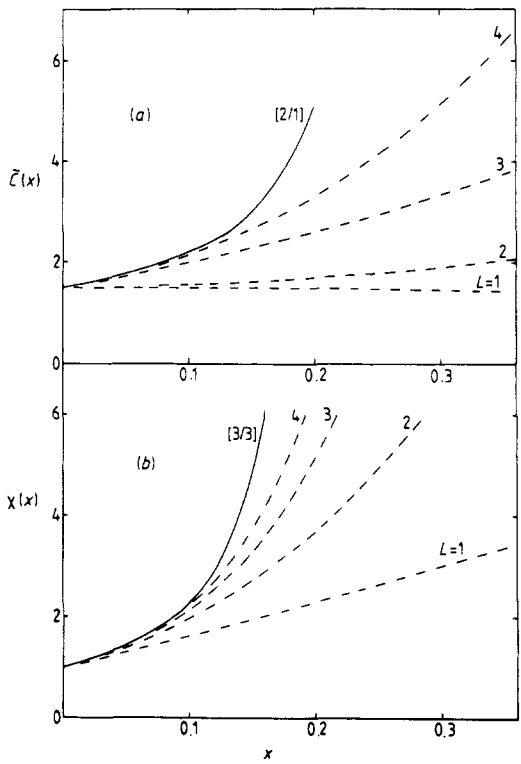

Figure 1. Graphs of (a) the specific heat and (b) the susceptibility of the (2+1)D Ising model on a triangular lattice. The full curve is the $[N/M]$ Padé approximant to the bulk limit, while the broken curves are ELCE approximants, labelled by their cut-off L.

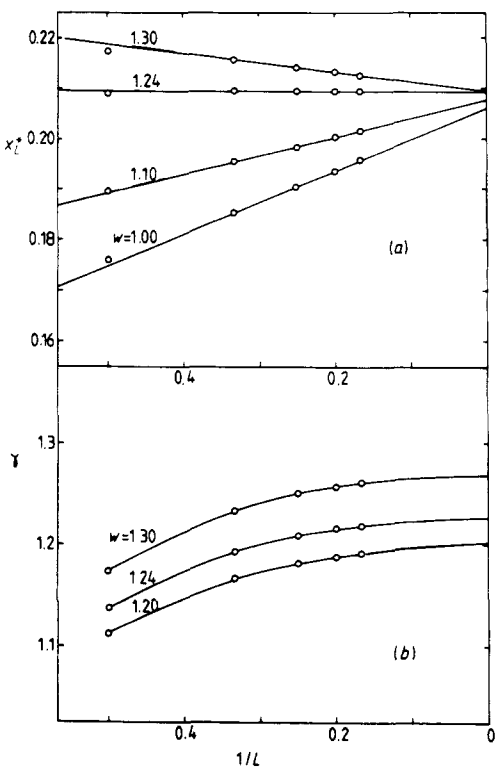

Figure 2. Scaling estimates of critical parameters for the (2+1)D Ising model on a triangular lattice, obtained from ELCE approximants to the susceptibility. Figure 2(a) shows the pseudo-critical points x_L^* graphed against $1/L$, where L is the cut-off; figure 2(b) shows the corresponding estimates of γ. Each curve is labelled by the value chosen for w, the scaling dimension.

estimates for the susceptibility converges rapidly and smoothly towards the bulk limit, represented by the Padé approximant curve. There is clear evidence of a divergence in the susceptibility around $x \simeq 0.2$.

The convergence of the sequence for the specific heat is also rapid at small x, but is not so smooth. There is a noticeable 'jump' between the estimates for $L=2$ and $L=3$, for instance. The reason for this is not hard to ascertain. Most topologies (e.g. the open chains) consisting of L links only contribute to the series for the vacuum energy at order x^{2L} and higher; but at $L=3$ we first meet a 'closed' topology, the triangle, which contributes at order x^3 rather than x^6, and so is unusually large†. This irregularity in the convergence of the ELCE estimates makes a scaling analysis very difficult: so we shall henceforth concentrate on the susceptibility results.

The question we would now like to address is whether the scaling properties of the ELCE sequence with cut-off L can be used to estimate critical parameters, in a way similar to the finite-size scaling methods (Fisher 1970, Fisher and Barber 1972, Hamer and Barber 1981a, b) used for finite-lattice sequences. There is a problem here, in that the finite-lattice estimates scale in a well known way, while the ELCE estimates do not. According to the finite-size scaling hypothesis (Fisher 1970, Fisher and Barber 1972, Hamer and Barber 1981a), the finite-lattice susceptibility at the critical point scales as

$$\chi_M \underset{M\to\infty}{\sim} M^{\gamma/\nu}, \tag{2.9}$$

where M is the linear dimension of the lattice. It is natural to assume that a similar form of scaling will be exhibited by the ELCE estimates, but the question arises as to what is the 'linear dimension' of a cluster of L links. The maximum dimension possible is $M \sim L$, for a straight chain of L links; and the minimum dimension possible is $M \sim L^{1/2}$, for a compact, 'space-filling' cluster in two space dimensions. We therefore expect the ELCE estimates to scale as

$$\chi_L \underset{L\to\infty}{\sim} L^{y\gamma/\nu} \tag{2.10}$$

where y is some unknown index in the range $\frac{1}{2} \leqslant y \leqslant 1$.

In I, a method was outlined to handle this situation, using a phenomenological renormalisation (Nightingale 1976) technique. This is based on a Roomany–Wyld (1980) 'beta function' for the susceptibility, defined as follows:

$$\beta_L(x) = \left(-w + \frac{\ln(\chi_L/\chi_{L-1})}{\ln(L/L-1)}\right) \Big/ [1 - x(\mathrm{d}/\mathrm{d}x)\ln(\chi_L\chi_{L-1})]. \tag{2.11}$$

This function has two important properties:

(i) The numerator vanishes at the point x_L^* such that

$$\chi_L(x_L^*)/\chi_{L-1}(x_L^*) = [L/(L-1)]^w. \tag{2.12}$$

Then if w is adjusted to match the proper scaling dimension $y\gamma/\nu$ (cf (2.10)), the sequence of values $\{x_L^*\}$ will converge to the critical point x_c as $L \to \infty$. This will also hold true, however, for a broad range of values about $y\gamma/\nu$. We may therefore treat w as an adjustable parameter.

† A similar anomaly is encountered in (3+1)D gauge theories, due to the closed, cubic topology (Irving and Hamer 1983a, b).

(ii) It is easy to check that if

$$\chi \sim (x_c - x)^{\gamma}, \tag{2.13}$$

then the asymptotic form of the beta function in the vicinity of the critical point is

$$\beta \sim w(x_c - x)/2x_c\gamma. \tag{2.14}$$

Thus the *slope* of the finite-cluster beta function β_L at the pseudo-critical point x_L^* may be used to provide an estimate of the true critical index γ; and the sequence of these estimates should converge to the exact value as $L \to \infty$.

Figures 2(*a*) and (*b*) display some results based on these ideas. In figure 2(*a*) the pseudo-critical points x_L^* are plotted as a function of cluster size L for various values of w. Each sequence can be quite well fitted by a straight line in the variable $1/L$, and extrapolated to the limit $L \to \infty$ to give a reasonably consistent estimate of the bulk critical point. Thus we find

$$x_c = 0.209 \pm 0.001. \tag{2.15}$$

The sequence converges most rapidly for $w = 1.24$, so we estimate

$$y\gamma/\nu = 1.24 \pm 0.01. \tag{2.16}$$

Figure 2(*b*) shows estimates of the critical index γ obtained from the slope of β_L at x_L^* via (2.14), as a function of L for various values of w. Choosing the 'correct' value $w = 1.24$ and extrapolating to the limit $L \to \infty$ via the curve illustrated, we arrive at a result

$$\gamma = 1.23 \pm 0.01. \tag{2.17}$$

The close similarity between the values (2.16) and (2.17) is presumably fortuitous.

A similar analysis of the square lattice data gives

$$x_c = 0.328 \pm 0.001, \tag{2.18}$$

$$y\gamma/\nu = 1.26 \pm 0.01, \tag{2.19}$$

$$\gamma = 1.24 \pm 0.01. \tag{2.20}$$

3. The mass gap

A true linked cluster expansion for the mass gap does not appear to be possible. A connected diagram expansion has been conjectured (Hamer and Irving 1984) for the mass gap of the bulk system, but end effects spoil the derivation for a finite lattice or finite cluster with free boundaries, and so the linked cluster expansion does not go through. But Nickel (1980a) has proposed another algorithm, which might be called an 'overlapping cluster' expansion, which is almost equally fast and efficient.

3.1. Cluster expansion for the mass gap

Nickel's argument (1980a) runs as follows. The standard perturbation theory expression for the energy of the first excited state may be written

$$\omega_1(x) = 2 + \frac{1}{N}\langle 1|V|1\rangle + \frac{1}{N}\langle 1|V\frac{P}{\omega_1 - H}V|1\rangle \tag{3.1}$$

where

$$|1\rangle = \sum_m \sigma_1(m)|0\rangle. \tag{3.2}$$

Here V is the perturbation operator $x\sum_{m,\hat{\mu}_i}\sigma_1(m)\sigma_1(m+\hat{\mu}_i)$, and P is a projection operator onto all states *except* those with one overturned spin. Now since the mass gap $F=\omega_1-\omega_0$ is intensive, while ω_0 is extensive, the contributions to F can only come from parts of the matrix elements that are proportional to N. We may therefore replace ω_1 by F in the denominator ω_1-H and write†:

$$F = 2+(1/N)\langle 1|V|1\rangle+(1/N)\Delta, \tag{3.3}$$

$$\Delta = \langle 1|V\frac{P}{F-H}V|1\rangle|_{\text{linear in } N}. \tag{3.4}$$

Now an iterative perturbation expansion for the quantity Δ can be written down in the usual manner, by expanding in powers of V:

$$\Delta = \left(\langle 1|V\frac{P}{F-H_0}V|1\rangle+\langle 1|V\frac{P}{F-H_0}V\frac{P}{F-H_0}V|1\rangle+\ldots\right)\Big|_{\text{linear in } N} \tag{3.5}$$

where $H_0=\Sigma_m(1-\sigma_3(m))$. Each term in this expression can be represented by a diagram, and each diagram spans a set of sites and links on the lattice, which may form a single linked cluster, or else a number of disconnected clusters (figure 3). A cluster expansion can thus be written down for Δ, very similar in form to that of § 2:

$$\Delta/N = \sum_{m,\beta_m} l'_{m,\beta_m}\varepsilon'_{m,\beta_m} \tag{3.6}$$

and

$$\Delta_{i,\beta_i} = \sum_{j,\beta_j}\tilde{C}^{i,\beta_i}_{j,\beta_j}\varepsilon'_{j,\beta_j}. \tag{3.7}$$

Here (m,β_m) denotes a set of m sites arranged in a topology β_m, which may be connected *or* disconnected; ε'_{m,β_m} is the contribution from all diagrams which span that topology, and Δ_{m,β_m} is the total of all diagrams which can be drawn on the set (m,β_m). The $\tilde{C}^{i,\beta_i}_{j,\beta_j}$ are embedding constants for topologies (j,β_j) within (i,β_i), and l'_{m,β_m} is the $O(N)$ term in the overall lattice constant for topology (m,β_m). We discuss in appendix 2 how these lattice constants and embedding constants may be calculated.

The algorithm then proceeds very much as in § 2. The quantity Δ_{i,β_i} can be calculated by a slight variation of the standard eigenvalue methods for any given cluster: we shall say a little more about this in § 3.3. Having found the Δ_{i,β_i}, one can invert (3.7) to find the ε'_{j,β_j}, and hence calculate the overall mass gap from (3.3) and (3.6). The algorithm is just as fast and efficient as that of § 2 for the ground-state energy, except that the list of topologies is longer by a factor of two or three for any given cut-off L.

3.2. Series results and analysis

The resulting series expansions in x for the mass gap on the square and triangular lattices are exhibited to order x^6 in table 1. This calculation took approximately three

† This manoeuvre may need further explanation. We assume that the Hamiltonian H is normalised so that the zeroth-order term in ω_0 vanishes, so that ω_0 is $O(Nx^2)$. If one then subtracts ω_0 from the denominator in (3.1), and expands in powers of x, then the only terms in Δ which are changed are $O(N^2)$ and higher.

Table 3. Padé analysis of the series for D log F in the (2+1)D Ising model. Notation as in table 2.

Order of Padé N	$[N/N-1]$	$[N/N]$	$[N/N+1]$
Square lattice			
1		0.324 (0.63)	0.329 (0.66)
2	0.336 (0.70)	0.330 (0.66)	0.330 (0.66)
3	0.330 (0.66)		
	Estimate: $x_c = 0.330 \pm 0.001$, $\nu = 0.66 \pm 0.02$		
Triangular lattice			
1		0.215 (0.69)	0.211 (0.66)
2	0.209 (0.64)	0.210 (0.65)	0.209 (0.62)
3	0.210 (0.65)		
	Estimate: $x_c = 0.210 \pm 0.001$, $\nu = 0.64 \pm 0.02$		

minutes on the VAX (excluding the generation of the list of topologies required), and was increasing by a factor of two or so at each order. The first four coefficients for the square lattice had previously been calculated by Pfeuty and Elliott (1971).

The results of a Padé approximant analysis of these series are shown in table 3. Hence we obtain estimates of the critical parameters:

$$x_c = 0.210 \pm 0.001, \qquad \nu = 0.64 \pm 0.02 \tag{3.8}$$

for the triangular lattice, and

$$x_c = 0.330 \pm 0.001, \qquad \nu = 0.66 \pm 0.02 \tag{3.9}$$

for the square lattice. These results for the critical points are consistent with those of § 2.2, but not so accurate.

3.3. Exact cluster expansions

As in § 2.3, one can now set out to generate an exact cluster expansion for the mass gap (which for convenience we shall again denote as ELCE, although the adjective 'linked' is inappropriate here). The strategy is the same as in § 2.3: one calculates *exact* expressions for the quantities Δ_{m,β_m} by matrix diagonalisation methods (Hamer and Barber 1981a, Roomany and Wyld 1980), for all clusters up to some convenient maximum size $m = M$, and then (3.6) and (3.7) are used to obtain an approximation to the bulk mass gap Δ.

The difficulty with this program is that the matrix to be diagonalised itself has to be generated in an iterative or self-consistent fashion for each cluster. Let D_{m,β_m} be the matrix whose lowest eigenvalue is Δ_{m,β_m}; then D_{m,β_m} has a block matrix form:

$$D_{m,\beta_m} = \begin{pmatrix} 0 & \langle 1|VP \\ PV|1\rangle & P(H_0' + V)P \end{pmatrix} \tag{3.10}$$

with notation as above, which is almost the same as the matrix H represented on the basis of states (in the odd spin-flip sector) belonging to the topology (m, β_m), except for the following differences. First, the entry $\langle 1|D|1\rangle$ has been set to zero, which merely eliminates terms through $O(x)$ from consideration. Secondly, all the single spin-flip

states have been summed into the state $|1\rangle$ as in (3.2), which is not normalised to unity. Finally, the diagonal piece H_0 of the Hamiltonian has been replaced by H_0', to be defined below. If H_0 were used, the usual iterative expansion for Δ_{m,β_m} would read:

$$\Delta_{m,\beta_m} = \langle 1|V\frac{P}{\Delta_{m,\beta_m}-H_0}V|1\rangle + \langle 1|V\frac{P}{\Delta_{m,\beta_m}-H_0}V\frac{P}{\Delta_{m,\beta_m}-H_0}V|1\rangle + \ldots \tag{3.11}$$

which is not what we want. To produce the expansion (3.5) we must 'renormalise' H_0 to a new diagonal matrix given by

$$H_0' = H_0 + sI, \tag{3.12}$$

$$s = \Delta_{m,\beta_m} - F. \tag{3.13}$$

The values of the overall mass gap F and the cluster contribution Δ_{m,β_m} which make up the shift s must then be calculated in an iterative or self-consistent fashion.

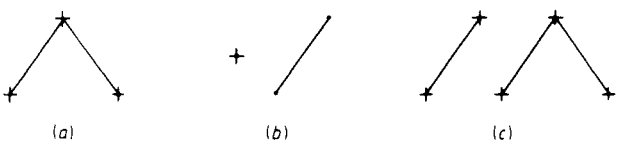

Figure 3. Examples of clusters which contribute to the expansion (3.6): (*a*) connected; (*b*), (*c*) disconnected. A cross denotes sites which may contain the initial spin excitation (NB a component consisting of a single site, as in (*b*), may only occur once and *must* contain the initial spin excitation, otherwise it cannot contribute to the high-temperature expansion).

A simple example may be useful at this point. Consider the cluster shown in figure 3(*b*). In this particular case, there is only one component to the initial state, $|1\rangle = |-++\rangle$, where + denotes an up spin and − denotes a flipped spin (see footnote to figure 3). The only excited state is $|2\rangle = |---\rangle$, and the matrix D can be represented on this basis as:

$$D_{(3(b))} = \begin{pmatrix} 0 & -x \\ -x & 6+\Delta_{(3(b))}-F \end{pmatrix} \tag{3.14}$$

whose eigenvalue is simply:

$$\Delta_{(3(b))} = -x^2/(6-F). \tag{3.15}$$

The series expansion of § 3.2 is simple to perform: at each order, one inserts the result obtained for F at the *previous* order into the perturbation series denominators, such as that in (3.15), in the standard iterative fashion. The exact cluster expansion is a little more difficult: one must modify the diagonal entries of the matrix D for each cluster, such as that in (3.14), in a self-consistent way in order to estimate Δ_{m,β_m} for each cluster plus the overall mass gap F. We have chosen to do this by the following algorithm.

(i) Choose a spread of five equally spaced estimates of the mass gap F.

(ii) For each cluster, choose a spread of five equally spaced estimates of the shift s in (3.12), and calculate the eigenvalue Δ_{m,β_m} of the matrix (3.10) corresponding to each such value of s.

(iii) For each value of F chosen at (i), find the value of Δ_{m,β_m} for which $s = \Delta_{m,\beta_m} - F$ by interpolation between the results calculated at (ii).

(iv) Inserting these values of Δ_{m,β_m} into equations (3.3)–(3.7), obtain an output value for the mass gap F. Find the point at which the input value of F is consistent with the output value by interpolation between the five values chosen at (i).

(v) Iterate the procedure once more, with a smaller spread of estimates, to check the stability and accuracy of the result.

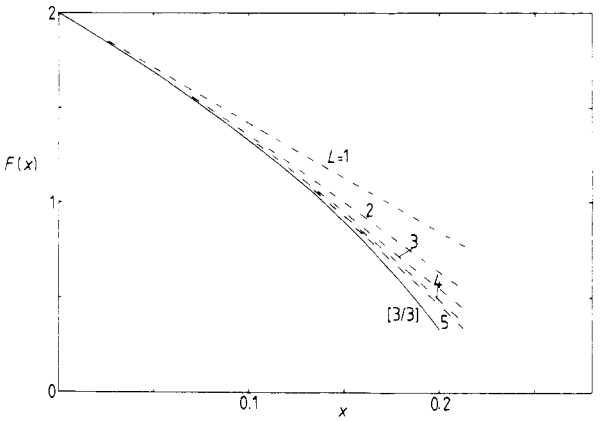

Figure 4. The mass gap of the (2+1)D Ising model on a triangular lattice. The full curve is a Padé approximant, and the broken curves are ELCE estimates, as in figure 1.

This procedure has been applied to the Ising model mass gap in (1+1)D and (2+1)D. Figure 4 displays the results for the (2+1)D model on the triangular lattice, as compared with the [3/3] Padé approximant to the mass gap. It can be seen that the ELCE approximants converge rapidly and smoothly to the bulk limit for $x < x_c$ and cut-off $L \leq 4$. For $L \geq 5$, the convergence begins to look more irregular, but we attribute this to the fact that our list of topologies was incomplete for $L \geq 4$, containing only those topologies needed to give series correct to $O(x^6)$. From the results for $L \leq 4$, the convergence appears to be linear in L for small x, as one might expect since the ELCE result coincides with the series expansion up to $O(x^L)$. At the critical point, the ELCE estimates appear to converge approximately as $L^{-0.5}$.

One might well ask why we have bothered to introduce these ELCE approximations at all, since the series Padé approximants provide as good or better estimates of the mass gap in the high-temperature region. The reason is that the ELCE is a topological expansion, rather than a perturbative one, and might be expected to converge to the correct physical limit at all couplings. The series Padé approximants are likely to prove rather unreliable in the weak coupling region of confining gauge theories, because of the proximity of the essential singularity at the continuum limit (Hamer 1979): it is our hope that the ELCE approximants will be more useful there. In the present work, our aim has been simply to show how such approximants for the mass gap may be calculated, and to show that they converge to the correct bulk limit.

A possible snag in this approach is that for some couplings there may not *exist* any real, self-consistent solutions for $\{\Delta_{m,\beta_m}\}$ and F. We have found possible evidence of this phenomenon for the (1+1)D Ising model beyond the critical coupling $x = 1$. It remains to be seen whether this will become a problem for the gauge theory case.

4. Discussion and conclusions

In this paper, some finite cluster algorithms due to Nickel (1980a) have been applied to the (2+1)D Ising model in the high-temperature regime. These methods are the most efficient that we know for generating perturbation series in Hamiltonian field theory. High-temperature series have been calculated for the vacuum energy and specific heat, the susceptibility, and the mass gap, on both square and triangular lattices in (2+1)D.

Padé analysis of these series resulted in the following estimates of the critical parameters: for the triangular lattice,

$$x_c = 0.209\,76 \pm 0.000\,15, \qquad \gamma = 1.247 \pm 0.005, \qquad \nu = 0.64 \pm 0.02, \tag{4.1}$$

and for the square lattice,

$$x_c = 0.3290 \pm 0.001, \qquad \gamma = 1.257 \pm 0.01, \qquad \nu = 0.66 \pm 0.02. \tag{4.2}$$

These estimates for the critical point are in close agreement with those of Yanase *et al* (1976), who had earlier calculated the susceptibility series. The results agree within errors with other analyses, e.g.

$$x_c = 0.329 \pm 0.001, \qquad \gamma' = 1.25 \pm 0.02, \tag{4.3}$$

for the square lattice, and

$$x_c = 0.2098 \pm 0.0002, \qquad \gamma' = 1.250 \pm 0.012, \tag{4.4}$$

for the triangular lattice, from a low-temperature series analysis (Marland 1981), and

$$x_c = 0.329 \pm 0.001, \qquad \nu = 0.635 \pm 0.005, \tag{4.5}$$

from a finite-lattice study on the square lattice (Hamer 1983). The results demonstrate, within errors, the universality of the critical indices γ and ν for the square and triangular lattices in (2+1)D, and for the 3D Ising model. The estimates are actually a little high compared with the accepted values for the 3D model (Le Guillou and Zinn-Justin 1980, Baker *et al* 1978)

$$\gamma = 1.241 \pm 0.002, \qquad \nu = 0.630 \pm 0.0015. \tag{4.6}$$

But this is usually the case for a standard high-temperature series analysis, and has been attributed to the influence of confluent singularities at the critical point (Nickel 1980b, Zinn-Justin 1981, Chen *et al* 1982). We have not made any attempt here to take these singularities into account. Our series could quite easily be extended by several more terms on a large main-frame computer, and it would then be worthwhile to perform a more careful analysis.

An exact linked cluster expansion (ELCE) based on Nickel's algorithms has also been studied. In this approach (Irving and Hamer 1983a), the contribution of each cluster topology is evaluated exactly by matrix techniques, rather than being expanded as a power series. We have demonstrated how to calculate ELCE approximants both for extensive quantities such as the susceptibility and for the mass gap, and shown that they converge to the correct bulk limit.

A study was also made of the scaling properties of the ELCE approximants to the susceptibility. As a function of the cut-off L (equal to the maximum number of links in the cluster), the ELCE approximants were found to converge linearly (i.e. like e^{-cL})

to the finite bulk limit for $x < x_c$. At the critical point x_c, the approximants scaled as

$$\chi_L \sim L^w \tag{4.7}$$

with

$$w = \begin{cases} 1.24 \pm 0.01 & \text{for the triangular lattice,} \\ 1.26 \pm 0.01 & \text{for the square lattice.} \end{cases} \tag{4.8}$$

A phenomenological renormalisation (Nightingale 1976, Roomany and Wyld 1980) technique, first introduced in I, was used to estimate the critical parameters:

$$x_c = 0.209 \pm 0.001, \qquad \gamma = 1.23 \pm 0.01, \qquad \text{for the triangular lattice,} \tag{4.9}$$

and

$$x_c = 0.328 \pm 0.001, \qquad \gamma = 1.24 \pm 0.01, \qquad \text{for the square lattice.} \tag{4.10}$$

These results agree well with the series values (4.1) and (4.2), but are somewhat less accurate. By analogy with the finite-size scaling properties of square lattices (Fisher 1970, Fisher and Barber 1972, Hamer and Barber 1981a), one might write

$$w = y\gamma/\nu, \tag{4.11}$$

whence one finds the scaling index y:

$$y = \begin{cases} 0.63 \pm 0.01 & \text{triangular lattice,} \\ 0.64 \pm 0.01 & \text{square lattice.} \end{cases} \tag{4.12}$$

But the significance of this index is not yet clear. From (4.12), it appears universal between different lattice structures; but it is probably *not* the same for different quantities, such as the susceptibility and the mass gap.

The characteristics of the ELCE approximants (Irving and Hamer 1983a) are intermediate between those of series (e.g. Padé) approximants and finite-lattice approximants (Hamer and Barber 1981a, b, Hamer 1983) as follows.

(i) The ELCE expansion is a topological, non-perturbative one, and so may be expected to converge to the correct physical result at all couplings, like the finite-lattice approximants. We have checked this for the vacuum energy in the present case (see also I), although the results are not shown here. The case of the mass gap is more problematical.

(ii) The ELCE expansion is biased towards one end of the coupling range, however, depending whether one chooses to base it on the high-temperature or low-temperature representation. Within the radius of convergence of the corresponding series, the ELCE approximants converge linearly to the bulk limit.

(iii) The scaling behaviour of the ELCE approximants at a critical point is qualitatively similar to that of the finite-lattice approximants. We have shown that the results may be analysed to provide quite good estimates of the critical parameters, in a favourable case. But in general one finds the ELCE approximants to be somewhat 'noisy', like the series coefficients, so that a scaling analysis will only work well when the ratio method (Gaunt and Guttmann 1974) also works well for the series coefficients. Thus an ELCE analysis of critical behaviour will in general be inferior to a series Padé analysis or a finite-lattice scaling analysis.

(iv) The advantage of the ELCE method is that it is practicable for models in three or four dimensions where exact finite-lattice methods are not feasible, and series methods break down, such as in the weak-coupling regime of a confining gauge theory.

It is in these latter regions that we expect the method to become useful: some initial applications have already been made to the Z_2 gauge model (Irving and Hamer 1983a) in (2+1)D, and the U(1) gauge model (Irving and Hamer 1983b) in (2+1)D and (3+1)D.

Acknowledgments

One of us (ACI) is grateful to the Royal Society for the award of a Commonwealth Bursary.

Appendix 1. Calculation of high-temperature embedding constants

The calculation of high-temperature, or 'weak', embedding constants has been quite fully discussed by Domb (1960, 1974) and Martin (1974). The topologies we are interested in consist of a set of points connected by bonds into a single linked cluster. They are embedded on the lattice so that points of the cluster correspond to sites of the lattice, and bonds correspond to links between neighbouring sites; and in the high-temperature (weak-embedding) case there are no restrictions on the embeddings except that points of the cluster cannot fall on top of each other.

The method we used to generate the embedding constants is a modification of that used in I for the low-temperature case.

(i) Linked clusters were generated on the lattice by the canonical labelling method of Martin (1974). Each cluster topology was characterised by an 'adjacency matrix' specifying all the links between neighbouring sites of the cluster.

(ii) Each cluster was placed in a class according to its topology, by the methods outlined in I. The number of clusters in each class gives the 'strong embedding' lattice constant for that topology, since at this stage each pair of neighbouring points is necessarily connected by a bond.

(iii) A representative of each topology class was 'stripped' to determine the sub-clusters it contains; by this means the embedding constants $C_{j,\alpha_j}^{l,\alpha_l}$ are obtained. In I, the stripping was done by systematically deleting *points* of the cluster, and looking for connected sub-clusters. In the present case, the stripping is done by deleting *bonds* in a similar fashion, to give the high-temperature embedding constants. If a connected sub-cluster is found with the same number of points as the original cluster, but with fewer bonds, then this configuration is added to the lattice constant l_{j,α_j} of the sub-cluster. Thus the lattice constants are converted to 'weak embedding' lattice constants, where neighbouring points are not necessarily connected by bonds.

We have checked that the resulting lattice constants agree with those given by Domb (1960), appendix III. The calculation of a list of topologies and their lattice constants for clusters through seven sites on the triangular lattice took approximately 20 minutes on the VAX 11/780, to generate 51 topologies with number of bonds $L \leqslant 6$. It may well be possible to streamline this process further.

Appendix 2. Calculation of weak embedding constants for disconnected clusters

To determine the mass gap, we need weak embedding constants for unlinked clusters (Domb 1960) as well as linked ones, such as those shown in figure 3. This calculation was performed by a further modification of the program outlined in appendix 1.

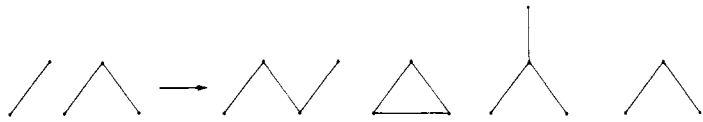

Figure 5. A typical disconnected topology (at left), and the topologies which may be formed when its components overlap (at right).

(i) Linked clusters were generated and classified by topology as in appendix 1.

(ii) A representative member of each topology class (i, α_i) was systematically stripped of its bonds as in (iii) of appendix 1. The embedding constants $C^{i,\alpha_i}_{j,\alpha_j}$ and weak lattice constants l_{j,α_j} were calculated as before for the linked clusters. At this stage, a list was kept of the 'stripped' adjacency matrices corresponding to each linked sub-cluster (j, α_j).

(iii) Next, all possible *combinations* of linked sub-clusters within the topology (i, α_i) were tested (up to appropriate cut-offs on size and number of sub-clusters). Each combination corresponds to a disconnected topology, which we shall denote (k, β_k). Tests were performed for the following conditions:

(a) None of the sub-clusters overlap, in which case the configuration must be included in the embedding constant $C^{i,\alpha_i}_{k,\beta_k}$.

(b) The sub-clusters overlap to span the *entire* original cluster (i, α_i), in which case the configuration contributes to an 'overlap constant' $O^{i,\alpha_i}_{k,\beta_k}$ defined as the number of ways the topology (k, β_k) can overlap so as to span (i, α_i). This will be used below to calculate the lattice constants.

(iv) Finally, each disconnected topology was tested as a 'parent' of other disconnected sub-topologies. Combining the embedding constants $C^{i,\alpha_i}_{k,\beta_k}$ for each linked component of (m, β_m), it is possible to deduce the overall embedding constant $C^{m,\beta_m}_{l,\beta_l}$ for disconnected topologies within other disconnected topologies. Similarly, one may deduce the overlap constant $O^{m,\beta_m}_{l,\beta_l}$ from those of the linked components. From this information, one can calculate the overall lattice constant for each disconnected topology, according to the formula†

$$l_{l,\beta_l} = -\sum_{m,\beta_m} l_{m,\beta_m} O^{m,\beta_m}_{l,\beta_l}, \tag{A2.1}$$

where now the sum includes both connected and disconnected topologies (m, β_m). We refer to Domb (1960) for a discussion of these constants. One explicit example may help to make things clear. Consider the topology shown at the left of figure 5. Contributions to its lattice constant (i.e. the coefficient of the order N term in its lattice embedding constant) come from configurations where the two components overlap to form the four topologies shown at right. Evaluating formula (A2.1), we obtain:

$$\begin{aligned} \text{lattice constant} &= -69\times 2 - 2\times 3 - 20\times 3 - 15\times 2 \\ &= -234 \end{aligned} \tag{A2.2}$$

where the contributions at the first line are in order of the four topologies in figure 5, and these lattice constants are for a triangular lattice.

We have checked that our lattice constants agree with those of Domb (1960), appendix III, table C. For the mass gap calculation to $O(x^6)$ on the triangular lattice, a list of 160 topologies was required, whose generation took 20–30 minutes on the VAX.

† Depending on conventions, there may be some extra symmetry factors involved here. We shall leave the determined reader to figure these out for himself.

References

Baker G, Nickel B G and Meiron D I 1978 *Phys. Rev.* B **17** 1365

Chen J-H, Fisher M E and Nickel B G 1982 *Phys. Rev. Lett.* **48** 630

Domb C 1960 *Adv. Phys.* **9** 149

—— 1974 in *Phase Transitions and Critical Phenomena* ed C Domb and M S Green, vol 3 (New York: Academic)

Elliott R J, Pfeuty P and Wood C 1970 *Phys. Rev. Lett.* **25** 443

Fisher M E 1970 in *Critical Phenomena, Proc. Int. School of Physics 'Enrico Fermi', Varenna, Course no 51* ed M S Green (New York: Academic)

Fisher M E and Barber M N 1972 *Phys. Rev. Lett.* **28** 1516

Fradkin E and Susskind L 1978 *Phys. Rev.* D **17** 2637

Gaunt D S and Guttmann A J 1974 in *Phase Transitions and Critical Phenomena* ed C Domb and M S Green, vol 3 (New York: Academic)

Hamer C J 1979 *Phys. Lett.* **82**B 75

—— 1983 *J. Phys. A: Math. Gen.* **16** 1257

Hamer C J and Barber M N 1981a *J. Phys. A: Math. Gen.* **14** 241, 259

—— 1981b *J. Phys. A: Math. Gen.* **14** 2009

Hamer C J and Irving A C 1984 *Nucl. Phys.* B **230** [FSIO] 336

Irving A C and Hamer C J 1983a *Nucl. Phys.* B to appear

—— 1983b *Nucl. Phys.* B to appear

Jullien R, Pfeuty P, Fields J N and Doniach S 1978 *Phys. Rev.* B **18** 3568

Le Guillou J C and Zinn-Justin J 1980 *Phys. Rev.* B **21** 3976

Marland L G 1981 *J. Phys. A: Math. Gen.* **14** 2047

Martin J L 1974 in *Phase Transitions and Critical Phenomena* ed C Domb and M S Green, vol 3 (New York: Academic)

Nickel B G 1980a unpublished

—— 1980b *Lecture Notes at the 1980 Cargèse Summer Institute on Phase Transitions* ed M Levy, J C Le Guillou and J Zinn-Justin (New York: Plenum 1982)

Nightingale M P 1976 *Physica* A **83** 561

Penson K A, Jullien R and Pfeuty P 1979 *Phys. Rev.* B **19** 4653

Pfeuty P and Elliott R J 1971 *J. Phys. C: Solid State Phys.* **4** 2370

Roomany H and Wyld H W 1980 *Phys. Rev.* D **21** 3341

Yanase A, Takeshige Y and Suzuki M 1976 *J. Phys. Soc. Japan* **41** 1108

Zinn-Justin J 1981 *J. Physique* **42** 783